Acceptor–Enhanced Local Order in Conjugated Polymer Films

ARTICLE *in* JOURNAL OF PHYSICAL CHEMISTRY LETTERS · MARCH 2013

Impact Factor: 7.46 · DOI: 10.1021/jz400333k

THE JOURNAL OF PHYSICAL CHEMISTRY Letters

Letter

pubs.acs.org/JPCL

Acceptor-Enhanced Local Order in Conjugated Polymer Films

Olga D. Parashchuk,[†,‡] Souren Grigorian,[§] Eduard E. Levin,[†,⊥] Vladimir V. Bruevich,[†,‡] Kirill Bukunov,[†,‡] Ilya V. Golovnin,[†,‡] Thomas Dittrich,[#] Kirill A. Dembo,[▽] Vladimir V. Volkov,[▽] and Dmitry Yu. Paraschuk*[,†,‡]

[†]Faculty of Physics, [‡]International Laser Center, and [⊥]Faculty of Chemistry, Lomonosov Moscow State University, 119991 Moscow, Russia

[§]Institute of Physics, University of Siegen, Emmy-Noether-Campus, Walter-Flex-Strasse 3, D-57068 Siegen, Germany

[#]Helmholtz-Zentrum Berlin, Hahn-Meitner-Platz 1, 14109 Berlin, Germany

[▽]Shubnikov Institute of Crystallography of the Russian Academy of Sciences, Leninskii prospekt 59, 119333 Moscow, Russia

Supporting Information

ABSTRACT: Disorder in conjugated polymers is a general drawback that limits their use in organic electronics. We show that an archetypical conjugated polymer, MEH-PPV, enhances its local structural and electronic order upon addition of an electronic acceptor, trinitrofluorenone (TNF). First, acceptor addition in MEH-PPV results in a highly structured XRD pattern characteristic for semicrystalline conjugated polymers. Second, the surface roughness of the MEH-PPV films increases upon small acceptor addition, implying formation of crystalline nanodomains. Third, the low-frequency Raman features of the polymer are narrowed upon TNF addition and indicate decreased inhomogeneous broadening. Finally, the photoinduced absorption and surface photovoltage spectroscopy data show that photoexcited and dark polymer intragap electronic states assigned to deep defects disappear in the blend. We relate the enhanced order to formation of a charge-transfer complex between MEH-PPV and TNF in the electronic ground state. These findings may be of high importance to control structural properties as they demonstrate an approach to increasing the order of a conjugated polymer by using an acceptor additive.

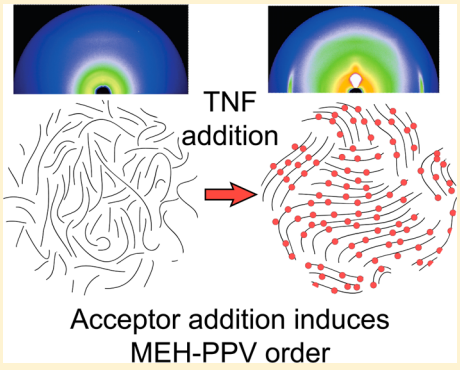

SECTION: Energy Conversion and Storage; Energy and Charge Transport

Organic electronics is expected to be based on easy processable, low-cost techniques for thin films fabricated from solution. However, preparation of ordered semiconducting films from solution is a challenge for modern film processing techniques as they were historically developed for nonconjugated polymers, which do not have semiconducting properties. The control of interchain interactions in conjugated polymer materials is of key importance to achieve appropriate nano- and microscale order that supports the key electronic properties, for example, efficient exciton transport and high charge mobility. Donor−acceptor blends of conjugated materials have been in the focus of active research for the past decade. In these blends, a bulk heterojunction (BHJ) can be formed that is the heart of modern organic solar cells. For efficient BHJ solar cells, the phase-separated donor and acceptor phases must form an interdigitating network, with the electron and hole mobilities being balanced. On the way to ordered polymer/fullerene blends, a number of approaches have been proposed at the stages of films preparation and their postprocessing. Different annealing techniques (e.g., solvent, thermal) have been developed for P3HT/PCBM blends to optimize the BHJ morphology after film preparation.[1] Using processing additives before film preparation as another promising approach to ordered polymer/fullerene BHJs has recently been proposed.[2−4]

However, it is generally accepted that polymer/fullerene interactions in the ground electronic state are too weak to influence the BHJ morphology and structural order. Although charge-transfer interaction (CTI) in the electronic ground state of the polymer/fullerene blends has recently been identified[5,6] and the high importance of the corresponding charge-transfer excited states for the BHJ photophysics has been highlighted,[7,8] there is still no evidence that this interaction can essentially influence the BHJ morphology. Moreover, the polymer order is usually not improved in donor−acceptor blends as compared with the pristine polymer.

At the same time, if the donor−acceptor CTI in the electronic ground state of the blend would be sufficiently strong as compared with other intermolecular interactions in the donor (acceptor) phase, this CTI could potentially be used to influence and maybe even control the BHJ order. Meanwhile, polymer/acceptor blends with seemingly far stronger CTI in

Received: February 14, 2013
Accepted: March 25, 2013
Published: March 25, 2013

the electronic ground state as compared with common polymer/fullerene blends have recently been found.[9−11] The archetypical conjugated polymer MEH-PPV has been shown to form pronounced intermolecular ground-state charge-transfer complexes (CTCs) in blends with low-molecular-weight organic acceptors, in particular, with trinitrofluorenone (TNF). These Mulliken-type CTCs are characterized by weak ground-state charge transfer (~0.2e$^-$)[12] that differentiates them from doped conjugated polymers in which the full electron transfer is implied. The excited CTCs have been found to play a key role in the photophysics of the blend, so that geminate recombination of charge-transfer excitons is much faster[13−15] than that in polymer/fullerene blends.[16] Moreover, CTI in MEH-PPV/TNF blends can also modify their ground-state properties.[11,17−19]

In this Letter, we investigate both structural and electronic ordering in MEH-PPV/TNF blends by using complementary X-ray diffraction, atomic force microscopy (AFM), Raman spectroscopy, and photophysical data. The latter are obtained with the use of photoinduced absorption (PIA) and surface photovoltage (SPV) spectroscopies that can probe long-lived and permanent (dark) charged states in the material, respectively. We explain the observed enhanced order by donor−acceptor interaction in the ground state of the blend resulting in formation of a CTC between MEH-PPV and TNF.

Figure 1 demonstrates 2D patterns measured by the grazing incidence X-ray diffraction (GIXD) technique for pristine MEH-PPV, 1:0.3 MEH-PPV/TNF, and 1:1 MEH-PPV/TNF films. The relation between the reciprocal space coordinates (Q_z and $Q_{x,y}$) and their out-of- and in-plane probing directions can be found elsewhere.[20] Corresponding in- and out-of-plane profiles from the 2D patterns are given in Figure 1S of the Supporting Information (SI). One can see that the MEH-PPV/TNF blends give a textured 2D GIXD pattern, whereas the pristine polymer shows a uniformly decreasing scattering signal without any clear diffraction features (Figure 1a). Addition of TNF results in clear in-plane and out-of-plane GIXD peaks, as seen in Figure 1b,c. The in-plane signal is observed at scattering vectors of 1.70 and 1.72 Å^{-1} that correspond to interplanar spacings (d_{010} spacings) of 3.7 and 3.65 Å for the 1:0.3 and 1:1 blends, respectively. We assign this spacing to the distance between TNF and MEH-PPV π-conjugated backbones in the face-to-face configuration. The strongest out-of-plane peak is observed at ~0.45 Å^{-1}, and the corresponding d_{100} spacing (~13 Å) is assigned to the side-chain length of MEH-PPV. The 2D GIXD patterns indicate that polymer chains in the blends have the edge-on configuration similar to that observed in polyalkylthiophenes.[21,22] Figure 2 shows the suggested polymer chain packing with TNF molecules sandwiched between the adjacent polymer plains. A number of weak powder-like diffraction rings observed in the 1:1 blend (Figure 1c) are assigned to randomly oriented TNF microcrystallites that appear in blends at TNF/MEH-PPV content higher that 0.3:1.[11,17] More detailed information on MEH-PPV packing in the blends by out-of-plane GIXD data is given in the SI. Briefly, we suggest coexistence of two packing motifs of polymer chains in the MEH-PPV/TNF blends (Figure 2). Assuming polymorphism with two orthorhombic unit cells, we suggest that, in one motif, the long side groups of different chains are oriented collinear (Figure 2a), and in other motif, the long side groups are oriented toward each other (Figure 2b), forming a bilayer structure.[23] As a result, the two packing motifs differ on the *a*-axis in their d_{100} and d'_{100} spacings (~13 and 24 Å). Note that the presence of polymer domains with different packing motifs was earlier assumed for pristine MEH-PPV.[23]

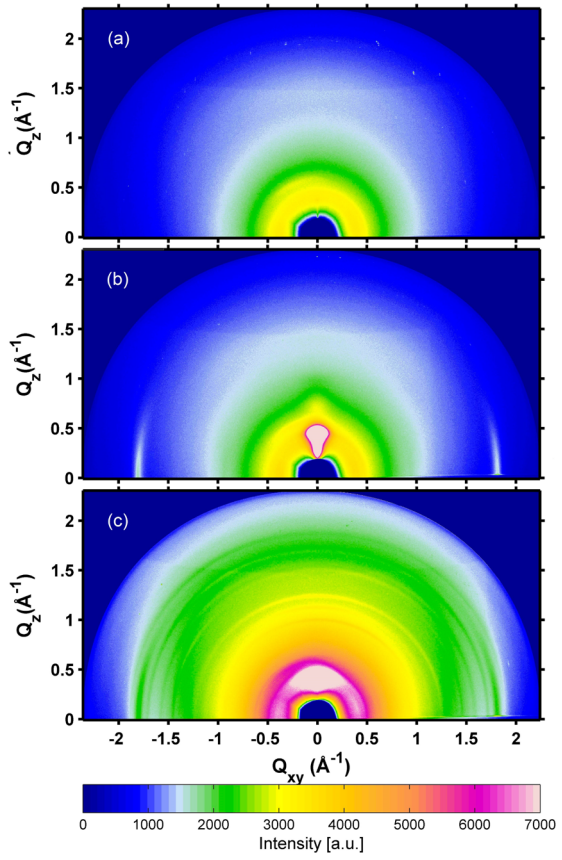

Figure 1. Two-dimensional GIXD patterns for pristine MEH-PPV (a), 1:0.3 MEH-PPV/TNF (b), and 1:1 MEH-PPV/TNF (c) films.

The nanoscale surface morphology of MEH-PPV/TNF blends was studied by AFM on films spin-cast from chlorobenzene on glass substrates. AFM images of pristine and blend films with low content of TNF are given in Figure 6S (SI). The pristine MEH-PPV film shows a very smooth surface with a root-mean-squared roughness of 0.84 nm (Figure 6Sa, SI) that is typical for amorphous polymers. Upon a small addition of TNF, the surface roughness of the blend strongly increases and reaches 1.67 nm, with the typical lateral size of the features being about 20−30 nm (Figure 6Sb, SI). We suggest that the surface morphology is hardly affected by the TNF phase in the blends with low content of TNF (<0.2). This is in accordance with the above X-ray data and also supported by the differential scanning calorimetry (DSC)[11] and Rayleigh scattering data[17] on MEH-PPV/TNF blends with various TNF content. The increased surface roughness in the blend could be attributed to aggregation of the conjugated segments involved in the CTC.

The low-frequency vibrational spectroscopy is a sensitive tool for probing intermolecular and interchain order. We have found the changes in the low-frequency Raman spectrum of MEH-PPV in the MEH-PPV/TNF blends in the spectral range below 400 cm^{-1}. The Raman data are given in Figure 7S (SI). They show that the Raman features' widths noticeably decrease with increasing TNF content. This is in parallel with the earlier observation of narrowing the high-frequency Raman band at ~1580 cm^{-1} in MEH-PPV/TNF blends.[12] Although at present

dx.doi.org/10.1021/jz400333k | J. Phys. Chem. Lett. 2013, 4, 1298−1303

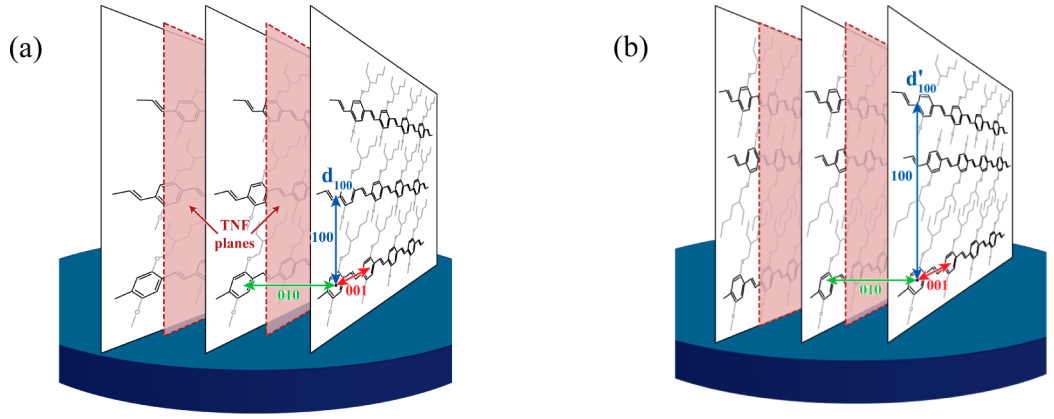

Figure 2. Proposed model for polymer chain packing in the MEH-PPV/TNF blends with short d_{100} (a) and long d'_{100} (b) spacings.

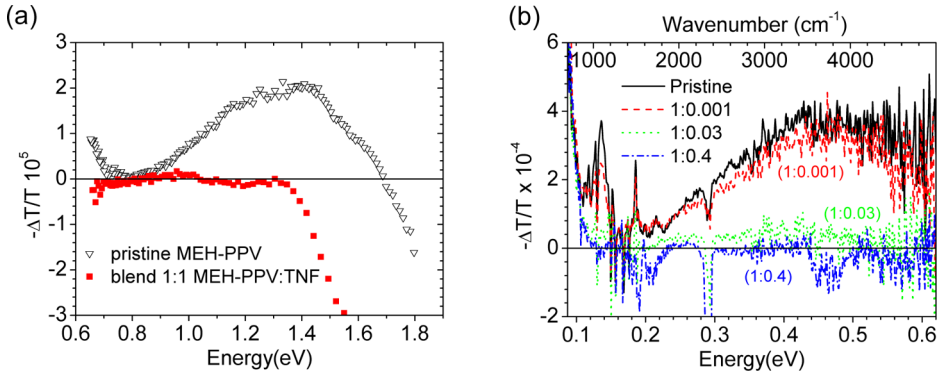

Figure 3. PIA spectra of pristine MEH-PPV and 1:1 MEH-PPV/TNF blend films in the near-IR (a) and mid-IR (b) spectral ranges. The negative PIA signals in panel (b) for the 1:0.4 blend in the 0.2 and 0.45 eV regions are due to the ambient water vapor, and features at ~0.29 eV are due to the ambient CO_2.

we do not assign the low-frequency Raman bands, the observed Raman band narrowing in the blends indicates decreased inhomogeneous broadening and is evidence of enhanced molecular order. Importantly, the Raman data are indicative of the order of the conjugated chains that determine the observed Raman response.

To characterize the electronic order in the blends, specifically defect states, we used photoinduced absorption (PIA) and surface photovoltage (SPV) spectroscopies. The former probes very long lived photoinduced charged states with a typical lifetime longer than 1 ms, and the latter was used in the Kelvin probe arrangement to probe dark defect states in the optical gap of the material. Figure 3 compares PIA spectra of pristine MEH-PPV and MEH-PPV/TNF films recorded in the near-IR (a) and mid-IR (b) spectral ranges, correspondingly. The near-IR PIA spectrum of the pristine MEH-PPV shows a broad band at ~1.3 eV assigned to long-lived charged states (polarons).[24] In addition, a shoulder below 0.7 eV is observed that is also a characteristic of the lower-energy polaron band at ~0.5 eV.[25] The intensity of these bands is quite low, which indicates a low yield of photogenerated charges in the pristine polymer. In contrast, in the blend, we did not observe any PIA that can be assigned to long-lived charged states (Figure 3). In fact, the blend PIA spectrum is dominated by bleaching of CTC absorption without any signs of intragap absorption. The bleaching signal both in the pristine polymer and blend can be assigned to the thermochromic shift of the polymer absorption edge.[26]

The same result, that is, the absence of long-lived photoinduced charges in the blend, also follows from our mid-IR PIA data. Figure 3b presents photoinduced FTIR absorption (PIA-FTIR) spectra of pristine MEH-PPV and MEH-PPV/TNF blended films. Characteristic signatures of charge photogeneration[25] are observed only for the pristine MEH-PPV and the blend with the lowest TNF concentration (1:0.001); both of the photoinduced vibrational bands are observed in the range of 0.1−0.19 eV, and the electronic in-gap absorption is observed at ~0.4 eV. The latter is assigned to the low-energy polaron band whose shoulder at ~0.7 eV was observed in the near-IR PIA data (Figure 3a). At the same time, MEH-PPV/TNF films with higher TNF content did not show any signatures of photoinduced charged states.

Note that the initial charge generation is very efficient in MEH-PPV/TNF blends as in the MEH-PPV/fullerene blends, as follows from the ultrafast PIA studies.[14,15] However, our PIA data indicate that addition of TNF to MEH-PPV strongly suppress long-lived charged excitations in the material. We explain this correlation as a consequence of the enhanced polymer order that is characterized by a lower concentration of deep traps for charges in the blends. Indeed, some conjugated polymers show this correlation. For example, highly ordered polyacetelyne in the form of nanoparticles (nanopolyacetelene) exhibits exactly the same trend, that is, the correlation of the enhanced order with the absence of long-lived charged excitations.[27,28]

The SPV technique directly probes spatially separated charges, in contrast to the PIA technique that does not give

dx.doi.org/10.1021/jz400333k | J. Phys. Chem. Lett. 2013, 4, 1298−1303

information about the spatial scale of charge separation. Figure 4 compares SPV spectra of pristine MEH-PPV and the MEH-PPV/TNF blend. The pristine MEH-PPV film demonstrates the SPV signal closely following its absorption spectrum starting at ~2 eV. In addition, the pristine MEH-PPV shows a broad subgap feature with the onset at ~0.9 eV. We assign this feature to deep dark states that generate mobile charges under optical excitation. As Figure 4 shows, in the blend, this intragap feature disappears, and the SPV spectrum more or less follows the blend absorption. In fact, addition of TNF to MEH-PPV extends the blend absorption into the MEH-PPV optical gap as a result of CTC formation.[9,29]

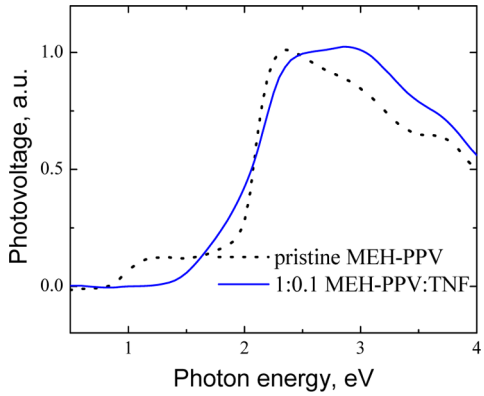

Figure 4. SPV spectra of MEH-PPV and MEH-PPV/TNF blended films recorded at room temperature in vacuo. A typical photovoltage was in the range of 0.1−0.15 V for all of the samples. The background signal below 1 eV was subtracted from the SPV spectra.

To summarize, the SPV data indicate that addition of TNF to MEH-PPV results in suppression of dark intragap states assigned to defects. The disappearance of these states at TNF addition is in parallel with the PIA data indicating suppression of long-lived photoinduced polaron states.

One may suggest that the enhanced structural and electronic polymer order will result in an increased charge mobility. The hole mobility in pristine polymer and blended films was measured using organic field effect transistors (see the SI). We found that the hole mobility in the blend is somewhat lower than that in the pristine film. These observations suggest that the correlation between crystallinity and mobility is not straightforward. The local crystallinity can induce multiple grain boundaries, and their inconsistency can cause less efficient charge transport.

The textured GIXD patterns and complementary observed nanodomains in the AFM images are characteristic features of semicrystalline conjugated polymers, for example, polyalkylthiophenes. Therefore, one can conclude that TNF addition in the nominally amorphous polymer MEH-PPV induces structural order resulting in formation of crystalline domains. We relate this ordering to donor−acceptor CTI in the electronic ground state of the blend. Specifically, as was suggested from the dynamic light scattering[30] and Raman data,[12] the CTC can link two conjugated segments via a polymer/acceptor/polymer $\pi-\pi$ interaction, so that the TNF molecules are sandwiched between the neighboring polymer chains, resulting in the in-plane GIXD peaks at a d spacing of 3.6 Å (in-plane peaks at higher $Q_{x,y}$ in Figure 1b,c). Furthermore, as follows from the Raman data on MEH-PPV/TNF blends, the CTC formation induces planarization of conjugated segments involved in the CTCs.[12] This planarization combined with the increased interchain interaction could facilitate chain aggregation in nanodomains.[18] Acceptor-induced chain aggregation can start in solution, as follows from our photoluminescence quenching data.[31] Importantly, addition of TNF to MEH-PPV also improves the electronic order, as can be concluded from the PIA and SPV data. Electronic ordering is implied as suppression of deep defect electronic states in the polymer. If these defects are conformational ones, for example, chain folding, planarization of the polymer chains could decrease their concentration. Possibly, the very high photooxidation stability observed in MEH-PPV/TNF blends[32] could be partly related to the improved electronic order, that is, to the lower concentration of chemically active sites with localized π-electron density. Nevertheless, the observed ordering in the blends occurs only in nanodomains that probably are surrounded by the disordered polymer phase. This suggestion is supported by the DSC studies on MEH-PPV/TNF blends[11] that did not show any clear features of a new macroscopic phase. In addition, the charge mobility did not increase in the blends, indicating that the macroscopic order was not improved. On the other hand, the hole mobility in alkyl-PPV/PCBM blends is strongly enhanced[33,34] as compared with that of the pristine polymer, and this observation may be related to very weak ground-state polymer/fullerene CTCs.[6,33] Meanwhile, relatively strong CTI in donor−acceptor blends appears to be detrimental for organic solar cells, resulting in low photocurrent because of very fast recombination of photoinduced charges (i.e., charge-transfer excitons) at the picosecond time scale.[15] Accordingly, the appropriate choice of the polymer/acceptor pair, tuning their interaction, and film processing conditions could possibly result in ordering at a larger scale that would be of high importance for organic electronic devices, specifically, for bulk heterojunction solar cells.

To summarize, the nominally amorphous polymer, MEH-PPV, can be both structurally and electronically ordered at the nanoscale with the use of an acceptor additive, TNF. We have related the enhanced order to the formation of CTC between MEH-PPV and TNF in the electronic ground state. Importantly, the ground-state donor/acceptor interaction mediated by the CTC is quite efficient to compete with polymer/polymer interactions, and this results in ordering the polymer chains involved in the CTC. These CTC features could be useful for tailoring the morphology in donor−acceptor blends used in organic photovoltaics.

EXPERIMENTAL METHODS

Samples. The polymer (MEH-PPV or MDMO-PPV, Sigma-Aldrich) and TNF were dissolved separately in chlorobenzene at concentrations in the range of 2−4 g/L. Blends were prepared by mixing the solutions of MEH-PPV and TNF with their molar ratio from 1:0.1 to 1:1 per repeat unit. Films were prepared on glass or silicon substrates by drop-casting or spin-casting at 1500 rpm.

X-ray Diffraction. GIXD studies of the drop-cast polymer films were carried out using synchrotron radiation at BL9 station of DELTA synchrotron, Dortmund (λ = 0.8267 Å). 2D images were taken by an image plate with 3450 × 3450 pixels of 100 μm size spaced at 55 cm from the sample and probed with a beam size of 0.5 × 1.5 mm^2. In order to enhance the X-ray signal from the polymer films and to suppress the background signal from the glass substrate, all of the scattering 2D patterns

dx.doi.org/10.1021/jz400333k | J. Phys. Chem. Lett. 2013, 4, 1298−1303

were measured at a shallow angle of 0.08°, close to the critical angle of the polymer films at 15 keV. X-ray diffraction (XRD) data were also collected in step-scan mode at room temperature using a $\theta-2\theta$ Bragg−Brentano RIGAKU D/max RC diffractometer operating with CuKα radiation and equipped with a graphite analyzer and a scintillation detector. XRD out-of-plane patterns were recorded in the specular scattering geometry ($\theta-2\theta$) and in the grazing incidence mode with a grazing angle of 1°. GIXD profiles of MDMO-PPV/TNF blends were measured in the out-of-plane scattering geometry using the laboratory source Seifert XRD 3003 PTS-HR (λ = 1.542 Å) at the University of Siegen. Small-angle scattering data were collected on the diffractometer "AMUR-K" with a linear position-sensitive detector "OD3-M" and a graphite monochromator (λ = 1.542 Å). A Kratky-type collimator was used with a sample to detector distance of 700 mm and a sample slit width of 0.2 mm to cover the range of scattering vectors 0.05−1.2 Å $^{-1}$.

Atomic Force Microscopy. The AFM images were obtained in tapping mode under ambient conditions using an Integra Spectra probe microscope (NT-MDT). NT-MDT NGS03 cantilevers (140 kHz) were used.

Photoinduced Absorption. In the PIA experiments, the pump beam was mechanically chopped, and the PIA signal in the probe channel was processed by a lock-in amplifier at a modulation frequency in the range of 30−100 Hz. In the probe channel, a tungsten halogen lamp to illuminate the sample, a monochromator, and solid-state photodetectors (Si and InGaAs) were used. A continuous wave frequency-doubled Nd:YAG laser radiating at 532 nm was used as a pump source with a typical intensity of 1 W/cm^2. For pristine MEH-PPV films, the PL was subtracted from the measured PIA signal, with the data being recorded under nitrogen flow. Drop-cast films at room temperature were studied. FTIR-PIA experiments were carried out using an Infralum FT-801 spectrometer with a MG-32A photodetector in ambient conditions with a resolution of 6 cm^{-1}. PIA-FTIR spectra were measured by accumulating IR transmission spectra with and without illumination during the equal time intervals (16 or 32 s). The data were averaged over large numbers of "light/dark" cycles to reach an appropriate signal-to-noise ratio, which usually took a few hours. Polymer films on BaF_2 substrates were illuminated by the second harmonic of a Nd:YAG CW laser (wavelength, 532 nm; intensity, 60 mW/cm^2) at ambient laboratory conditions. To check the substrate heating effect, the following experiment was performed. We placed in the sample unit of the spectrometer a sample and a clear BaF_2 substrate heated up to 60 °C and recorded the absorption spectra until it got cold to room temperature. Heating affects the BaF_2 absorption below 1000 cm^{-1}, which makes the heating effect readily observable.

Surface Photovoltage Spectroscopy. To record SPV spectra, a Kelvin probe arrangement was used. The SPV signal was measured between the film sample and the Au grid vibrating reference probe. A quartz prism monochromator equipped with a tungsten halogen lamp was used as the light source in the spectral range of 0.5−4 eV. The sample was placed in the vacuum cryostat (~10^{-5} mbar). All measurements were done at room temperature.

■ ASSOCIATED CONTENT

Ⓢ Supporting Information

X-ray, Raman, AFM, and OFET data. This material is available free of charge via the Internet at http://pubs.acs.org.

■ AUTHOR INFORMATION

Corresponding Author

*Telephone: +7-495-9392228. Fax: +7-495-9393113. E-mail: paras@physics.msu.ru.

Notes

The authors declare no competing financial interest.

■ ACKNOWLEDGMENTS

The authors thank S. A. Zapunidi for contribution to the PIA spectroscopy studies and V. A. Dyakov for AFM studies at the early stage of this work, S. N. Polyakov for help in X-ray studies, S. A. Ponomarenko for substrates for OFETs, A. S. Sizov for assistance with OFET measurements, the BL9 beamline staff at Delta, Dortmund, and V. M. Kobryanskii and U. Pietsch for fruitful discussions. This work was supported in part by the M.V.Lomonosov Moscow State University Program of Development and by the Russian Ministry of Education and Science (contract #11G34.31.0055 and Agreement #8082).

■ REFERENCES

(1) Campoy-Quiles, M.; Ferenczi, T.; Agostinelli, T.; Etchegoin, P. G.; Kim, Y.; Anthopoulos, T. D.; Stavrinou, P. N.; Bradley, D. D. C.; Nelson, J. Morphology Evolution via Self-Organization and Lateral and Vertical Diffusion in Polymer:Fullerene Solar Cell Blends. *Nat. Mater.* **2008**, *7*, 158−164.

(2) Lee, J. K.; Ma, W. L.; Brabec, C. J.; Yuen, J.; Moon, J. S.; Kim, J. Y.; Lee, K.; Bazan, G. C.; Heeger, A. J. Processing Additives for Improved Efficiency from Bulk Heterojunction Solar Cells. *J. Am. Chem. Soc.* **2008**, *130*, 3619−3623.

(3) Peet, J.; Cho, N. S.; Lee, S. K.; Bazan, G. C. Transition from Solution to the Solid State in Polymer Solar Cells Cast from Mixed Solvents. *Macromolecules* **2008**, *41*, 8655−8659.

(4) Pivrikas, A.; Stadler, P.; Neugebauer, H.; Sariciftci, N. S. Substituting the Postproduction Treatment for Bulk-Heterojunction Solar Cells Using Chemical Additives. *Org. Electron.* **2008**, *9*, 775−782.

(5) Goris, L.; Haenen, K.; Nesladek, M.; Wagner, P.; Vanderzande, D.; De Schepper, L.; D'Haen, J.; Lutsen, L.; Manca, J. V. Absorption Phenomena in Organic Thin Films for Solar Cell Applications Investigated by Photothermal Deflection Spectroscopy. *J. Mater. Sci.* **2005**, *40*, 1413−1418.

(6) Benson-Smith, J. J.; Goris, L.; Vandewal, K.; Haenen, K.; Manca, J. V.; Vanderzande, D.; Bradley, D. D. C.; Nelson, J. Formation of a Ground-State Charge-Transfer Complex in Polyfluorene/[6,6]-Phenyl-C-61 Butyric Acid Methyl Ester (PCBM) Blend Films and Its Role in the Function of Polymer/PCBM Solar Cells. *Adv. Funct. Mater.* **2007**, *17*, 451−457.

(7) Veldman, D.; Meskers, S. C. J.; Janssen, R. A. J. The Energy of Charge-Transfer States in Electron Donor−Acceptor Blends: Insight into the Energy Losses in Organic Solar Cells. *Adv. Funct. Mater.* **2009**, *19*, 1939−1948.

(8) Vandewal, K.; Tvingstedt, K.; Gadisa, A.; Inganas, O.; Manca, J. V. On the Origin of the Open-Circuit Voltage of Polymer−Fullerene Solar Cells. *Nat. Mater.* **2009**, *8*, 904−909.

(9) Bakulin, A. A.; Khodarev, A. N.; Martyanov, D. S.; Elizarov, S. G.; Golovnin, I. V.; Paraschuk, D. Y.; Arnautov, S. A.; Nechvolodova, E. M. Charge Transfer Complexes of a Conjugated Polymer. *Dokl. Chem.* **2004**, *398*, 204−206.

(10) Bakulin, A. A.; Elizarov, S. G.; Khodarev, A. N.; Martyanov, D. S.; Golovnin, I. V.; Paraschuk, D. Y.; Triebel, M. M.; Tolstov, I. V.; Frankevich, E. L.; Arnautov, S. A. Weak Charge-Transfer Complexes Based on Conjugated Polymers for Plastic Solar Cells. *Synth. Met.* **2004**, *147*, 221−225.

(11) Paraschuk, D. Y.; Elizarov, S. G.; Khodarev, A. N.; Shchegolikhin, A. N.; Arnautov, S. A.; Nechvolodova, E. M. Weak Intermolecular Charge Transfer in the Ground State of a π-Conjugated Polymer Chain. *JETP Lett.* **2005**, *81*, 467−470.

(12) Bruevich, V. V.; Makhmutov, T. S.; Elizarov, S. G.; Nechvolodova, E. M.; Paraschuk, D. Y. Raman Spectroscopy of Intermolecular Charge Transfer Complex between a Conjugated Polymer and an Organic Acceptor Molecule. *J. Chem. Phys.* **2007**, *127*, 104905.
(13) Bakulin, A. A.; Zapunidy, S. A.; Pshenichnikov, M. S.; van Loosdrecht, P. H. M.; Paraschuk, D. Y. Efficient Two-Step Photogeneration of Long-Lived Charges in Ground-State Charge-Transfer Complexes of MEH-PPV Doped with Fullerene. *Phys. Chem. Chem. Phys.* **2009**, *33*, 7324−7330.
(14) Bakulin, A. A.; Martyanov, D.; Paraschuk, D. Y.; van Loosdrecht, P. H. M.; Pshenichnikov, M. S. Charge-Transfer Complexes of Conjugated Polymers as Intermediates in Charge Photogeneration for Organic Photovoltaics. *Chem. Phys. Lett.* **2009**, *482*, 99−104.
(15) Bakulin, A. A.; Martyanov, D. S.; Paraschuk, D. Y.; Pshenichnikov, M. S.; van Loosdrecht, P. H. M. Ultrafast Charge Photogeneration Dynamics in Ground-State Charge-Transfer Complexes Based on Conjugated Polymers. *J. Phys. Chem. B* **2008**, *112*, 13730−13737.
(16) Deibel, C.; Strobel, T.; Dyakonov, V. Role of the Charge Transfer State in Organic Donor−Acceptor Solar Cells. *Adv. Mater.* **2010**, *22*, 4097−4111.
(17) Elizarov, S. G.; Ozimova, A. E.; Paraschuk, D. Y.; Arnautov, S. A.; Nechvolodova, E. M. Laser Light Scattering as a Probe of Phase Separation in Donor−Acceptor Conjugated Polymer Films. *Proc. SPIE* **2006**, *6257*, 293−302.
(18) Parashchuk, O. D.; Bruevich, V. V.; Paraschuk, D. Y. Association Function of Conjugated Polymer Charge-Transfer Complex. *Phys. Chem. Chem. Phys.* **2010**, *12*, 6021−6026.
(19) Parashchuk, O.; Sosorev, A.; Bruevich, V.; Paraschuk, D. Threshold Formation of an Intermolecular Charge Transfer Complex of a Semiconducting Polymer. *JETP Lett.* **2010**, *91*, 351−356.
(20) Joshi, S.; Pingel, P.; Grigorian, S.; Panzner, T.; Pietsch, U.; Neher, D.; Forster, M.; Scherf, U. Bimodal Temperature Behavior of Structure and Mobility in High Molecular Weight P3HT Thin Films. *Macromolecules* **2009**, *42*, 4651−4660.
(21) Chabinyc, M. L. X-Ray Scattering from Films of Semiconducting Polymers. *Polym. Rev.* **2008**, *48*, 463−492.
(22) Shabi, T. S.; Grigorian, S.; Brinkmann, M.; Pietsch, U.; Koenen, N.; Kayunkid, N.; Scherf, U. Enhancement in Crystallinity of Poly(3-hexylthiophene) Thin Films Prepared by Low-Temperature Drop Casting. *J. Appl. Polym. Sci.* **2012**, *125*, 2335−2341.
(23) Jeng, U.; Hsu, C.-H.; Sheu, H.-S.; Lee, H.-Y.; Inigo, A. R.; Chiu, H. C.; Fann, W. S.; Chen, S. H.; Su, A. C.; Lin, T.-L. Morphology and Charge Transport in Poly(2-methoxy-5-(2′-ethylhexyloxy)-1,4-phenylenevinylene) Films. *Macromolecules* **2005**, *38*, 6566−6574.
(24) Smilowitz, L.; Sariciftci, N. S.; Wu, R.; Gettinger, C.; Heeger, A. J.; Wudl, F. Photoexcitation Spectroscopy of Conducting-Polymer−C_{60} Composites — Photoinduced Electron-Transfer. *Phys. Rev. B* **1993**, *47*, 13835−13842.
(25) Wei, X.; Vardeny, Z. V.; Sariciftci, N. S.; Heeger, A. J. Absorption-Detected Magnetic-Resonance Studies of Photoexcitations in Conjugated-Polymer/C_{60} Composites. *Phys. Rev. B* **1996**, *53*, 2187−2190.
(26) Bruevich, V. V.; Osotov, M. O.; Paraschuk, D. Y. Thermal Vibrational Disorder of a Conjugated Polymer in Charge-Transfer Complex. *J. Chem. Phys.* **2009**, *131*, 094906.
(27) Paraschuk, D. Y.; Kulakov, T. A.; Kobryanskii, V. M. Photoinduced Neutral Solitons up to Room Temperature in Soluble *trans*-Polyacetylene. *Phys. Rev. B: Condens. Matter* **1994**, *50*, 907−913.
(28) Smilowitz, L.; Sariciftci, N. S.; Hagler, T.; Pakbaz, K.; Heeger, A. J.; Kobryanskii, V. Photoinduced and Electroabsorption Spectroscopy of a New, Stable and Soluble Polyacetylene Blend. *Synth. Met.* **1993**, *55*, 159−164.
(29) Ozimova, A. E.; Bruevich, V. V.; Dittrich, T.; Paraschuk, D. Y. Enhanced Photostability and Red−NIR Photosensitivity of Conjugated Polymer Charge-Transfer Complexes. *Macromol. Symp.* **2010**, *296*, 138−143.
(30) Parashchuk, O. D.; Laptinskaya, T. V.; Paraschuk, D. Y. Macromolecular Dynamics of Conjugated Polymer in Donor−Acceptor Blends with Charge Transfer Complex. *Phys. Chem. Chem. Phys.* **2011**, *13*, 3775−3781.
(31) Sosorev, A. Y.; Parashchuk, O. D.; Zapunidy, S. A.; Kashtanov, G. S.; Paraschuk, D. Y. Intrachain Aggregation of Charge-Transfer Complexes in Conjugated Polymer:Acceptor Blends from Photoluminescence Quenching. *J. Phys. Chem. C* **2013**, DOI: 10.1021/jp4000158.
(32) Golovnin, I. V.; Bakulin, A. A.; Zapunidy, S. A.; Nechvolodova, E. M.; Paraschuk, D. Y. Dramatic Enhancement of Photo-Oxidation Stability of a Conjugated Polymer in Blends with Organic Acceptor. *Appl. Phys. Lett.* **2008**, *92*, 243311.
(33) Tuladhar, S. M.; Poplavskyy, D.; Choulis, S. A.; Durrant, J. R.; Bradley, D. D. C.; Nelson, J. Ambipolar Charge Transport in Films of Methanofullerene and Poly(phenylenevinylene)/Methanofullerene Blends. *Adv. Funct. Mater.* **2005**, *15*, 1171−1182.
(34) Mihailetchi, V. D.; Koster, L. J. A.; Blom, P. W. M.; Melzer, C.; De Boer, B.; Van Duren, J. K. J.; Janssen, R. A. J. Compositional Dependence of the Performance of Poly(*p*-phenylene vinylene): Methanofullerene Bulk-Heterojunction Solar Cells. *Adv. Funct. Mater.* **2005**, *15*, 795−801.